# Extreme positive allometry of animal adhesive pads and the size limits of adhesion-based climbing

David Labonte[*1], Christofer J. Clemente[2], Alex Dittrich[3], Chi-Yun Kuo[4], Alfred J. Crosby[5], Duncan J. Irschick[6] & Walter Federle[7]

[1,7]Department of Zoology, University of Cambridge, Cambridge, United Kingdom
[2]School of Science and Engineering, The University of the Sunshine Coast, Australia
[3]Department of Life Sciences, Anglia Ruskin University, Cambridget, United Kingdom
[4,6]Biology Department, University of Massachusetts Amherst, USA
[5]Department of Polymer Science and Engineering, University of Massachusetts Amherst, USA

Organismal functions are size-dependent whenever body surfaces supply body volumes. Larger organisms can develop strongly folded internal surfaces for enhanced diffusion, but in many cases areas cannot be folded so that their enlargement is constrained by anatomy, presenting a problem for larger animals. Here, we study the allometry of adhesive pad area in 225 climbing animal species, covering more than seven orders of magnitude in weight. Across all taxa, adhesive pad area showed extreme positive allometry and scaled with weight, implying a 200-fold increase of relative pad area from mites to geckos. However, allometric scaling coefficients for pad area systematically decreased with taxonomic level, and were close to isometry when evolutionary history was accounted for, indicating that the substantial anatomical changes required to achieve this increase in relative pad area are limited by phylogenetic constraints. Using a comparative phylogenetic approach, we found that the departure from isometry is almost exclusively caused by large differences in size-corrected pad area between arthropods and vertebrates. To mitigate the expected decrease of weight-specific adhesion within closely related taxa where pad area scaled close to isometry, data for several taxa suggest that the pads' adhesive strength increased for larger animals. The combination of adjustments in relative pad area for distantly related taxa and changes in adhesive strength for closely related groups helps explain how climbing with adhesive pads has evolved in animals varying over seven orders of magnitude in body weight. Our results illustrate the size limits of adhesion-based climbing, with profound implications for large-scale bio-inspired adhesives.

The evolution of adaptive traits is driven by selective pressures, but can be bound by phylogenetic, developmental and physical constraints [1]. Integrating evolution and biomechanics provides a powerful tool to unravel this complex interaction, as physical constraints can often be predicted easily from first principles [2]. The influence of physical constraints is especially evident in comparative studies across organisms which differ substantially in size [3, 4, 5, 6]. For example, Fick's laws of diffusion state that diffusive transport becomes increasingly insufficient over large distances, explaining the development of enlarged surfaces for gas and nutrient exchange (e. g. leaves, roots, lungs, gills, guts) and integrated long-distance fluid transport systems (e. g. xylem/phloem, circulatory systems) in larger animals and plants. How these systems change with size is determined by physical constraints [7, 8, 9]. Although 'fractal' surface enlargements are possible without disrupting other body functions, strong positive allometry can conflict with anatomical constraints. For example, structural stability demands that animals should increase the cross-sectional area of their bones in proportion to their body weight, but excessively thick leg bones can compromise other physiological functions and hamper locomotion [3, 10, 11].

Adhesive pads are another example of an adaptive trait subject to size-dependent physical constraints. These systems allow animals to climb smooth vertical or inverted surfaces, thereby opening up new habitats. Adhesive pads have evolved multiple times independently within arthropods, reptiles, amphibians and mammals, and show impressive performance: they are rapidly controllable, can be used repeatedly without any loss of performance, and

function on rough, dirty and flooded surfaces [12]. This performance has inspired a considerable amount of work on technical adhesives that mimic these properties [13]. A key challenge for both biological and bio-inspired adhesive systems is to achieve size-independent performance [14, 15, 16], i. e. the maximum sustainable adhesion force, $F$, should be proportional to the mass to be supported, $m$. For vertically climbing animals, $F$ is the product of the maximum adhesive stress, $\sigma$, and the adhesive pad area, $A$, each of which may change with mass ($A \propto m^a$ and $\sigma \propto m^b$), so that constant size-specific attachment performance requires:

$$m \propto A\sigma \propto m^a m^b \rightarrow a + b \approx 1 \qquad (1)$$

where $a$ and $b$ are the scaling coefficients for $\sigma$ and $A$ in relation to body mass, respectively. If animals maintain geometric similarity when increasing in size, $A$ would scale as $m^{2/3}$ , so that the adhesion per body weight for large geckos ($m \approx 100\,\mathrm{g}$) is expected to be approximately $10^{7/3} \approx 200$ times smaller than for tiny mites ($m \approx 10\,\mu\mathrm{g}$) if the pads' adhesive strength $\sigma$ remained unchanged ($b = 0$). Large animals can only circumvent this problem by (i) developing disproportionally large adhesive pads ($a > 2/3$), and/or (ii) systematically increasing the maximum force per unit pad area ($b > 0$). How do large climbing animals achieve adhesive forces equivalent to their body weight?

Using the simple biomechanics argument outlined above as a framework, we here provide a comparative analysis of the allometry of adhesive pad area across 225 species, covering more than seven orders of magnitude in weight — almost the entire weight range of animals climbing with ad-
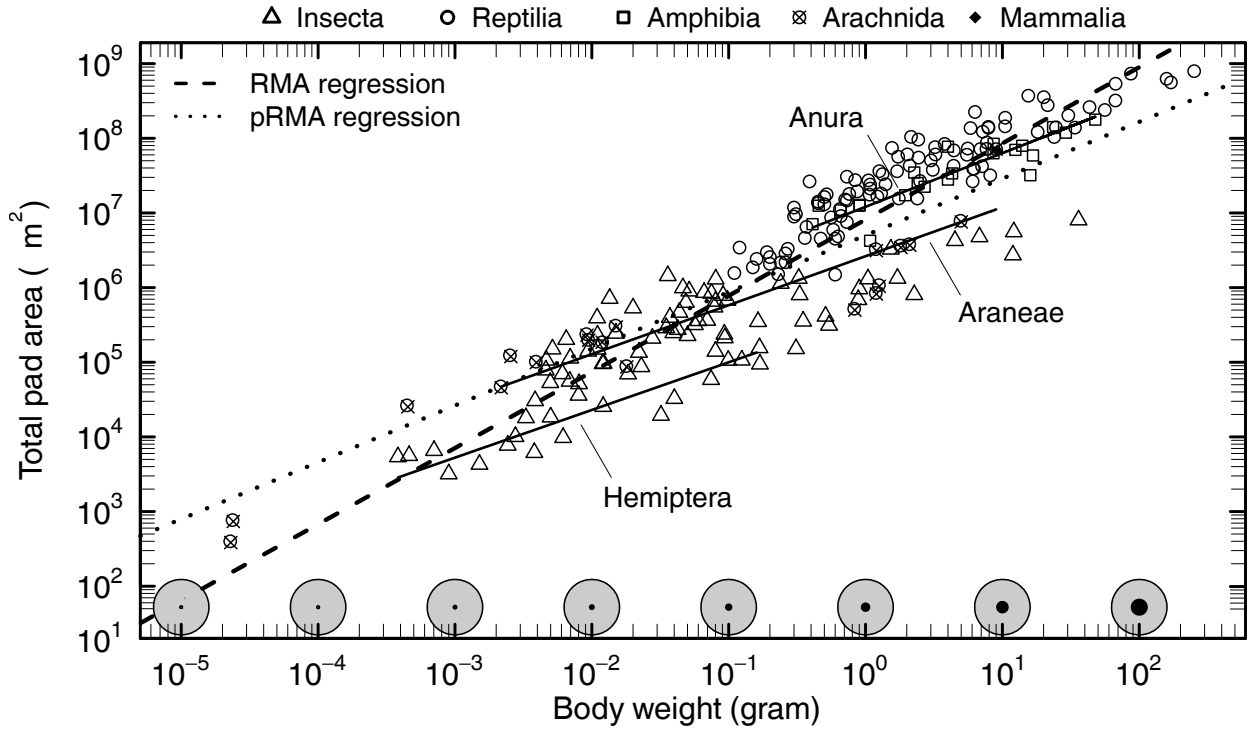
1

Figure 1: Allometry of pad area for 225 species, ranging from $\approx 20\,\mu$g to $\approx 200$ g in body weight. Across all taxa, pad area was directly proportional to body weight (reduced major axis regression, RMA, dashed line). The increase in the fraction (black circles) of the total available surface area (grey circles) required to accommodate this disproportionate change is schematically illustrated along the bottom axis, assuming that a climbing animal of 80 kg has a total surface area of 2m$^2$, comparable to a human of 80 kg and 180 cm, and that body surface area is approximately isometric. Strikingly, scaling relationships were significantly less steep within closely related groups (representative solid lines from RMA regressions), and closer to isometry when phylogenetic relationships were accounted for (phylogenetic RMA regression, dotted line).

hesive pads — and including representatives from all major groups of adhesion-based climbers.

## Results and Discussion

### Scaling of adhesive pad area

Across all taxa, adhesive pad area showed extreme positive allometry and scaled as $A \propto m^{1.02}$ (reduced major axis regression (RMA); see fig. 1 and tab. 1 for detailed statistics), an increase sufficient to compensate for the predicted loss of weight-specific adhesion, even if adhesive strength remained unchanged. Thus, adhesive pads occupy a relatively larger fraction of the body surface area in larger animals. Within closely related taxonomic groups, however, pad area grew more slowly with body mass, indicating a strong phylogenetic signal (see fig. 1 and 2).

When evolutionary relationships were accounted for, the observed scaling coefficient decreased dramatically, and was almost consistent with isometry (fig. 1, 2 and tab. 1). This systematic change of allometric coefficients with taxonomic rank suggests that phylogenetic inertia impedes a disproportionate increase of pad area within closely related groups (fig. 2 and 3 A). Our results thus add to a body of evidence suggesting that the evolutionary flexibility of allometric slopes is low and larger changes in particular traits are mainly achieved by shifts of the allometric elevation [18, 19].

Removal of the influence of body size by analysing the residuals (termed 'relative pad area' in the following) of a phylogenetic reduced major axis regression (pRMA) allowed us to further investigate at what taxonomic level major shifts in relative pad area occurred, separating the effects of size and ancestry. Relative pad area differed strongly between vertebrates and arthropods, but comparatively little variation existed within these groups (fig. 3 A). More than 58% of the variation in residual pad area was explained by differences between vertebrates and arthropods (nested ANOVA, $F_{1,173}$=845, p<0.001, see tab. 2), so that body weight and phylum alone accounted for more than 90% of the total variation in pad area. Rather than being driven solely by variation in body size, differences in relative pad area appear to be tied to characteristic features of the corresponding phyla, such as, for example, the presence or absence of multiple distal pads (toes) per leg (fig. 3 B,C). However, we also found evidence for differences in relative pad area within lower taxonomic ranks. For example, members of the gecko genus *Sphaerodactylus* had considerably smaller pads than other Gekkotan lizards, whereas *Gekko* lizards had particularly well-developed pads (based on their relative pad area, fig.3 A). In insects, hemimetabolous orders had smaller relative pad areas than holometabolous orders (see fig.3 A). Adhesive pads can allow access to arboreal habitats [20, 21, 22], but they may come at the cost of reduced locomotor performance in situations where no adhesion is required [23, 24]. Thus, the multiple independent losses, gains, and reductions of adhesive pads in amphibians, insects, lizards and spiders

Table 1: Results for generalised least squares and reduced major axis regressions describing the relationship between $\log_{10}$(adhesive pad area) (in $\mu m^2$) and $\log_{10}$(mass) (in g) across all taxa. Covariance in pad area and body mass between related species was either ignored (uncorrected) or accounted for (corrected). Pagel's lambda is a statistic measuring the strength of phylogenetic signal ($\lambda$=1 indicates that the trait evolves like Brownian motion along the phylogeny, whereas $\lambda$=0 indicates that the trait is not correlated with phylogeny [17].). Numbers in brackets give approximate 95% confidence intervals of the estimated parameters where available.

| Uncorrected | Elevation | Slope | Pagel's $\lambda$ |
|---|---|---|---|
| Reduced major axis | | | |
| Pad area against mass | 6.91 (6.84, 6.98) | 1.02 (0.97, 1.07) | 0 (fixed) |
| Mass against pad area | -6.76 (-7.08, -6.44) | 0.98 (0.93, 1.03) | 0 (fixed) |
| Generalised least squares | | | |
| Pad area against mass | 6.88 (6.80, 6.94) | 0.95 (0.9, 1) | 0 (fixed) |
| Mass against pad area | -6.29 (-6.61, -5.96) | 0.91 (0.86, 0.95) | 0 (fixed) |
| Corrected | Elevation | Slope | Pagel's $\lambda$ |
| Reduced major axis | | | |
| Pad area against mass | 6.54 (6.47, 6.62) | 0.78 (0.74, 0.83) | 0.93 (fitted) |
| Mass against pad area | -8.38 (-8.77, -7.99) | 1.28 (1.21, 1.36) | 0.93 (fitted) |
| Generalised least squares | | | |
| Pad area against mass | 6.44 (6.28, 6.61) | 0.70 (0.66, 0.75) | 0.90 (fitted) |
| Mass against pad area | -7.54 (-7.97, -7.10) | 1.13 (1.06, 1.20) | 0.83 (fitted) |

[25, 26, 27, 28] likely reflect the ecological, behavioural and taxonomic diversity within these groups [29, 30].

## The size-limits of adhesion-based climbing

Strong positive allometry of non-convoluted body structures in organisms ranging in size over many orders of magnitude is difficult to achieve, owing to simple anatomical constraints. For example, bone mass in terrestrial animals is predicted to increase with mass$^{4/3}$ to maintain constant bone stress levels, but this would require unrealistic relative bone masses for larger mammals (scaling up an 8-gram shrew with ca 4% bone mass would produce a rather unfortunate 8-tonne elephant with 400% bone mass). The actual scaling coefficient is inevitably smaller ($\approx 1.1$) [31, 10], and alternative strategies have evolved to limit bone stresses [11].

Maintaining a pad area proportional to body weight in animals ranging from $10^{-5}$ to $10^2$ grams requires extraordinary morphological changes: assuming otherwise isometric animals, the proportion of the total body surface area specialised as adhesive pad needs to increase by a factor of $10^{7/3} \approx 200$. This extreme shape change may impose a size limit for adhesion-based climbing. Scaling up the relative pad area of arthropods and small vertebrates to a human of 180 cm body length and 80 kg body mass would result in an adhesive pad area of $\approx 10^{6.91} \cdot 80000^{1.02} \approx 0.81\,\mathrm{m}^2$, approximately 2/5 of the total available body surface area ($\approx 2\,\mathrm{m}^2$, [33]). The required morphological changes, if at all possible, would thus be enormous, and difficult to achieve over short evolutionary timescales. Our results therefore indicate that phylogenetic inertia restricts the 'design space' for evolution at least at higher taxonomic levels. Larger animals within closely related taxa must therefore either cope with a size-related decrease in their attachment ability, or develop alternative strategies to compensate for it. Recent studies on tree frogs and ants revealed that pad adhesive strength can vary systematically with size, resulting in an almost body size-independent attachment abilities
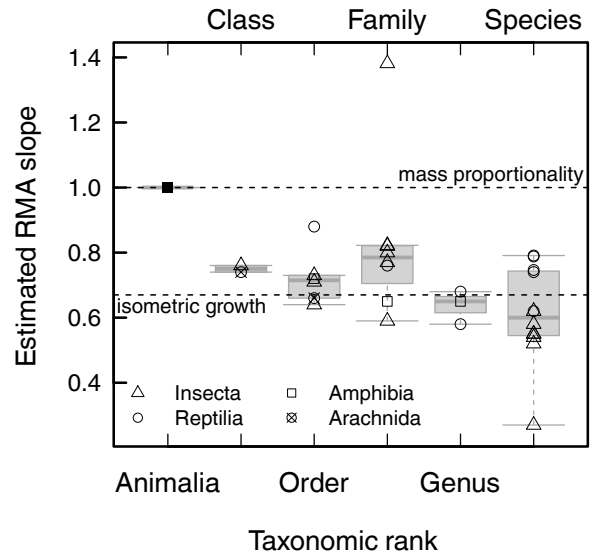


Figure 2: Change in pad allometry with taxonomic rank. For example, the slope of the regression line for Araneae in fig. 1 is one data point for the rank 'order'. Allometric coefficients decreased systematically, from mass-proportionality across all animals to isometry within genera and species. Data for the species-level allometry are from [32, 16].
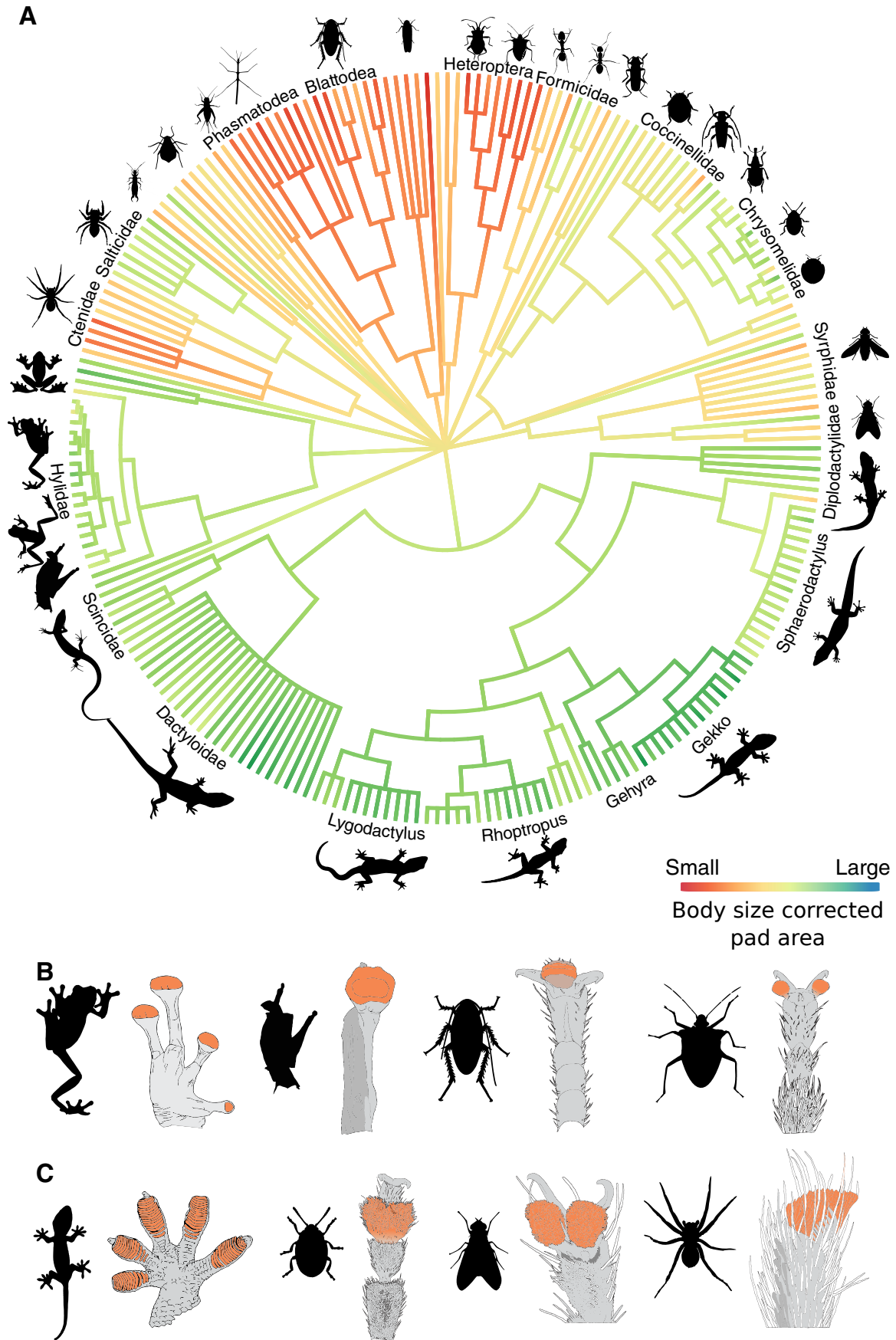
Figure 3: (A) Overview of the diversity of taxa examined in this study. Branch lengths do not reflect time or base pair substitutions (see methods). Branches are coloured according to a maximum likelihood estimate of the ancestral state of relative pad area (i. e. the residuals from a log-log regression of pad area against body weight), visualising systematic differences in relative pad area between arthropods and vertebrates. All values apart from tip states are only approximate and are not used to support any conclusions (see methods). (B & C) Cartoons depicting footpad morphology for representative groups within the phylogeny shown above with smooth and hairy adhesive pads. Projected pad area is highlighted in orange for each representative (see methods).

4

Table 2: Results for a nested ANOVA on the residuals of a phylogenetic reduced major axis regression. $\eta^2$ is the variance in residual pad area accounted for the by the different taxonomic levels, and most of the variation occurs between phyla.

| Tax. level | df | Mean squares | F | p-value | $\eta^2$ |
|---|---|---|---|---|---|
| Phylum | 1 | 40.25 | 845.16 | $< 0.001$ | 0.58 |
| Class | 3 | 0.41 | 8.55 | $< 0.001$ | 0.02 |
| Order | 12 | 1.02 | 21.43 | $< 0.001$ | 0.18 |
| Family | 35 | 0.22 | 4.52 | $< 0.001$ | 0.11 |
| Residuals | 173 | 0.05 | | | |

despite a near-isometric growth of pad area [34, 16]. Here, we extend these studies to investigate whether such adaptations are also present above species or genus level.

Figure 4 shows whole-body adhesion per pad area plotted against body weight for 17 frog species from 4 families and 12 genera [35, 36, 37, 38]. All adhesion measurements were conducted using a tilting platform, and are thus comparable across studies. Over two orders of magnitude in body weight, adhesion force per unit area increased with $m^{0.3}$ (RMA slope 0.3, 95% confidence interval (CI): (0.2, 0.43), generalised least-squares (GLS) slope 0.19, 95% CI: (0.08, 0.31), sufficient to achieve body size-independent adhesive performance despite an approximately isometric growth of pad area (RMA slope 0.74, 95% CI: (0.62, 0.87), GLS slope 0.70, 95% CI: (0.58, 0.83)). In contrast to our results for the allometry of pad area, this relationship remained virtually unchanged when phylogenetic relationships were accounted for, indicating that pad performance directly responded to selective pressures unconstrained by phylogenetic history (phylogenetic RMA slope 0.28, 95% CI: (0.2, 0.42), phylogenetic GLS slope 0.17, 95% CI: (0.070.27), see fig. 4).

Together, our results provide strong evidence that two different strategies have evolved to deal with the physical challenges of a larger body size. These strategies have been adopted at different taxonomic levels, highlighting how phylogenetic and physical constraints can influence the evolution of adaptive traits. Across distantly related groups, leg morphology is sufficiently different to accommodate large differences in relative pad area. Within closely related groups, where anatomical constraints result in a scaling of pad area closer to isometry, some taxa appear to have increased their pads' adhesive efficiency with size. The mechanisms underlying this increase in adhesive strength are still unclear, but may be of considerable interest for the development of large-scale bio-inspired adhesives. Various hypotheses have been proposed [37, 14, 16], but still remain to be tested.

## Force scaling and the evolution of 'hairy' adhesive pads

Arzt et al (2003) suggested that large animals with hairy adhesive pads have evolved higher hair densities to increase their pads' adhesive strength, an idea derived from the assumption that adhesive forces scale with the width of individual hair tips [39]. Assuming *isometric growth* of the total pad area, Arzt et al. predicted that hair density
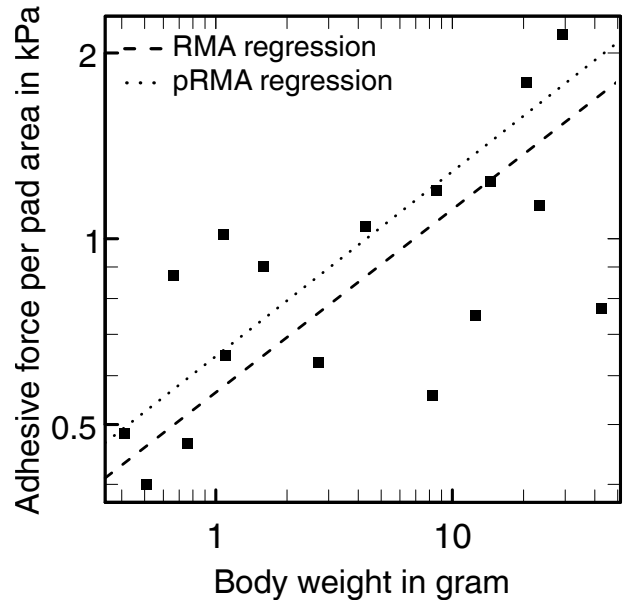


Figure 4: Adhesive force per area in 17 tree frog species increased with body mass, indicating that larger species possess more efficient pads. In contrast to the allometry of pad area, this result was not significantly influenced by phylogeny.

would need to increase with $m^{2/3}$ in order to achieve constant mass-specific adhesion, in agreement with the data presented (but see ref. [40] which showed that adhesive hair density increased with body mass only when species were treated as independent data points, but not when phylogeny was considered). However, our data show that total pad area is *directly proportional* to body mass across distantly related taxa, so that a constant hair density would suffice. In addition, there is no experimental evidence that the adhesive strength of animal adhesive pads increases with decreasing size of individual contacts [41, 16]. Thus, it appears unlikely that 'force scaling' has played an important role in the evolution of fibrillar adhesive systems [42].

Adhesive pads constitute a prime model system for studying the link between morphology, performance and fitness [43]. Further mechanistic and comparative studies are needed to elucidate the factors driving the evolution of these structures, and may ultimately allow us to mimic their properties with synthetic adhesives.

## Materials and Methods

### Data collection

Data were either collected by the authors or extracted from references [44, 45, 46, 47, 48, 49, 50, 51, 52, 35, 53, 54, 55, 56, 41, 57, 58, 59, 60, 61, 36, 37, 62, 63, 64, 65, 66, 67, 68, 69, 70, 71, 29, 72, 73, 74, 75, 76, 38, 77, 78, 79, 80, 81, 82, 83, 84, 85, 16, 86].

Arthropod specimens were collected around Cambridge (UK), Brisbane (Australia), or obtained from the Cambridge Phasmid Study Group. All arthropods were identified [87, 88, 89], and their live weight was recorded (ME5, resolution 1 $\mu$g, max 5 g or 1202 MP, resolution 0.01 g, max 300 g, both Sartorius AG, Goettingen, Germany). Attach-

ment pads were photographed either with a Canon EOS (Canon, Tokyo, Japan) mounted on a stereo microscope (MZ16, Leica Microsystems Ltd., Heidelberg, Germany), or by using scanning electron microscopy (SEM) for large and small specimens, respectively. Some pads were imaged whilst in contact with glass, visualised using the stereo-microscope with coaxial illumination. For SEM imaging, individual legs were dried, mounted on stubs, sputter-coated at 65 mA for 10-20 s (K575X turbo-pump sputter, Quorum Technologies, Sussex, UK) and examined with a field emission gun SEM at a beam voltage of 5 kV (Leo Gemini 1530VP, Carl-Zeiss NTS GmbH, Oberkochen, Germany).

Data on toepad-bearing gecko species were collected from live animals kept in the Irschick lab laboratory (under an Institutional Animal Care and Use (IACUC) protocol 2012–0064 from the University of Massachusetts at Amherst to DJ Irschick), and preserved specimens from the American Museum of Natural History and the Museum of Comparative Zoology at Harvard University. For each specimen, photos of one fore foot were obtained by pressing it tightly against the glass plate of an Epson Perfection V500 Photo Scanner (Seiko Epson Corp., Owa, Suwa, Nagano, Japan) next to a ruler and taking a digital scan. The total toepad area across all digits was measured using ImageJ v1.49r [90]. We also measured snout-vent-length ($\pm 1$ mm) from each individual using a clear plastic ruler. Where possible, we measured multiple conspecific individuals, and used the mean as the species value.

Literature data were taken from the papers' text or tables, or were extracted from figures using Web-PlotDigitizer 3.3 (WPD, developed by Ankit Rohatgi (http://arohatgi.info/WebPlotDigitizer), or ImageJ v1.49m. We tested the performance of WPD with an x-y plot of 20 random numbers between 1 and 1000 (x) and 0.01 and 10 000 (y) on a log-log scale, and found an accuracy of $\approx 0.6\%$ for the raw data.

We used live body weights where available, and interpolated live weight from body length where necessary, using established scaling relationships [40]. A list of the included species can be found in the supplemental material.

## Adhesive pad area

Animals attach to smooth surfaces by employing specialised attachment pads on their legs. These pads are either covered with dense arrays of fibrils ('hairy pads'), or are macroscopically unstructured ('smooth pads'). In order to compare pad areas across different taxa and pad morphologies, the following assumptions were made:

1. *'Projected' pad area is the most meaningful measure of contact area in comparative studies.* Projected pad area is the surface area of the foot specialised specifically for generating adhesion and friction [91]. In a fibrillar pad, inevitably only a fraction of this area comes into surface contact, i. e. the 'real' contact area is significantly smaller than the projected contact area.

2. *All animals employ a similar fraction of their available pad area when maximum performance is required.* It is unclear what fraction of the available pad area is

employed by animals of different size [92, 93, 16], and systematic studies are lacking. However, the small number of direct contact area observations available strongly suggest that animals often use the entire area of their adhesive pads [91, 94], i. e. that they are not 'overbuilt'. We thus assume that all climbing pads are designed so that their whole area can be used in critical situations.

3. *Adhesive performance is dominated by distal pads.* Insects can have several attachment pads per leg. There is strong evidence that these pad types differ in their morphology, as well as in their performance and function during locomotion [44, 91, 70, 65, 16]. Many insects do not employ their distal pads when no adhesion is required [44, 95, 96, 97, 65, 98], whereas during inverted climbing, only distal pads are in surface contact [83]. Accordingly, insects with ablated distal pads cannot cling upside down to smooth surfaces [44, 98]. Distal pads thus appear to be true 'adhesive pads' [83]. Proximal pads, in contrast, can be 'non-sticky', and may be designed as non-adhesive friction pads [99, 100]. The distal pads are usually part of the pretarsus, but some insects lack a pre-tarsal pad. In these insects, the distal tarsal pad can show similar morphological specialisations [101, 102]. Proximal pads are mainly found in arthropods, but they may also be present in frogs [35, 103]. As the contribution of proximal pads to adhesion is unclear and likely variable, we exclude them for this study. In most insects, the total proximal pad area is between 3-5 times larger than the distal pad area, and pad area is still positively allometric even when proximal pads are included (reduced major axis regression slope between 0.8-0.9).

4. *The variation of pad area/adhesive strength between different legs/toes and sexes of the same species, and the variation introduced by the animals' ecology is independent and randomly distributed with respect to body weight.* Several studies have shown that the size, morphology and performance of attachment devices can depend on the ecological niche occupied by the animals [104, 20, 59, 29, 22]. Variation can also occur between sexes [105, 70, 106], different legs or toes [20, 84], or even between populations of the same species occupying different habitats [24]. For this study, we assume that because of the large number of samples and the wide range of body sizes included, any bias introduced by these factors can be ignored.

5. *Adhesive performance of 'wet' and 'dry' pads is comparable.* Dynamic adhesive pads are frequently categorised as 'wet' or 'dry'. However, there is no evidence for a functional difference between these two pad types [107], and indeed maximal adhesive stresses are comparable [16].

As some of the data used in this study originate from different groups, we quantified the consistency of pad area measurements among researchers. A selection of SEM images (three hairy, and seven smooth pads) were given to 10 scientists who independently measured nominal pad

area. We found an average coefficient of variation of $17 \pm 9\%$, which was independent of the animals' body weight (ANOVA, $F_{1,8}=0.067$, p=0.8). Scaling relationships calculated with this dataset did not vary significantly across scientists (slope: likelihood ratio statistic= 0.38; elevation: Wald statistic=1.21, both df=9 and p>0.9).

## Phlyogenetic and statistical analyses

In order to account for the non-independence of data from related species, we first formed groups within which adhesive pads are likely homologous, based on their position on the leg and their structure (i. e. hairy vs. smooth pads). These groups are (1) Squamata, (2) Anura, (3) Araneae, (4) mites with smooth pads, (5) mites with hairy pads, (6) insects with tarsal hair fields (e. g. some Coleoptera and Raphidioptera), (6) insects with smooth pulvilli (e. g. some Hemiptera), (7) insects with hairy pulvilli (e. g. some Diptera), (8) insects with unfoldable arolia (some Hymenoptera), (8) insects with non-eversible arolia (e. g. some Polyneoptera, Hemiptera and Lepidoptera), (9) insects with specialised distal euplantula (some Polyneoptera), (10) insects with tibial pads (e. g. some aphids). These groups were all connected directly to the root of the tree, so that analogous structures share no branch, and thus the respective elements in the error covariance matrix of our linear models are zero [108]. Within this groups, we assembled a tree topology from phylogenies published for the constituent groups (Anura [109], Squamata [110], Aranae [28], Insecta [111], Blattodea [112], Coleoptera [113], Diptera [114], Hemiptera [115, 116], Hymenoptera [117, 118]. As statistically supported branch lengths were not available, comparative phylogenetic procedures which allow for more complex evolutionary models, such as Ornstein-Uhlenbeck models [119, 120], were not feasible. Instead, we performed phylogenetic generalised least squares on 10.000 trees with randomised branch lengths that were rendered ultrametric via a correlated rate model [121]. In order to account for the uncertainty of the phylogenetic error covariance structure, Pagel's $\lambda$ was estimated simultaneously via a maximum likelihood optimisation [17, 122]. The fitted coefficients were normally distributed, with a coefficient of variation below 1% (see fig. S1 in Supplementary Information). For simplicity, we report results for an ultrametric tree calculated from a tree with all branch lengths set to 1.

All analyses involving pad area and weight were performed on $\log_{10}$-transformed values, and with the the the routines implemented in the R packages nlme v.3.1-118, ape v.3.1-1, and phytools v.0.3-93 in R v.3.1.3 [123, 124]. There is some controversy as to whether (reduced) major axis or ordinary least squares regression is more appropriate for estimating allometric coefficients from data containing both 'measurement' and 'biological' error [125, 126, 18, 127, 19]. We thus report results for both techniques, and note that the key results of this study hold independent of what regression model is applied.

An alternative method to account for relatedness is to monitor the change of the estimated parameters as one moves up in taxonomic rank. We performed multiple reduced major axis regressions across all taxa, and separately within the taxonomic levels class, order, family and genus

(for example, all Hymenoptera provide one allometric slope data point within the level 'order'). Within the taxonomic levels, groups were only included if the weight range of the available species exceeded a factor of 3, and if data for at least 4 different groups from the next sub-level were available (e. g. an order was included if at least four families were represented).

In order to visualise the effect of evolutionary history on body size-corrected pad area, residuals from a phylogenetic reduced major axis regression were used to estimate maximum likelihood ancestral states for all nodes and along the branches via the method described in [128]. These values are only rough estimates, first because we do not have statistically supported branch lengths, second because the species sampling in our phylogeny is incomplete, third because we do not account for the influence of relative pad area on diversification rate, and fourth, because only shared ancestors among lower taxonomic ranks possessed adhesive pads. Ancestral state estimates are solely used to visualise systematic differences at the tip-level, and no conclusions are based on them.

## Scaling of pad performance in tree frogs

All data are from whole-animal force measurements, conducted using a tilting platform. In total, we extracted data for pad area and body weight for 17 species belonging to 4 families from references [35, 36, 37, 38]. The phylogenetic tree underlying the phylogenetic regressions was extracted from the detailed phylogeny in [109], and is shown in fig. S2 in the Supplementary Information.

## Appendix

The following species were included:

**Amphibia: Anura**, Dendrobatidae: *Mannophryne trinitatis* (Garman, 1887), Hemiphractidae: *Flectonotus fitzgeraldi* (Parker, 1933), Hylidae: *Dendropsophus microcephalus* (Cope, 1886); *Dendropsophus minusculus* (Rivero, 1971); *Dendropsophus minutus* (Peters, 1872); *Hyla cinerea* (Schneider, 1799); *Hyla versicolor* LeConte, 1825; *Hypsiboas boans* (Linnaeus, 1758); *Hypsiboas crepitans* (Wied-Neuwied, 1824); *Hypsiboas geographicus* (Spix, 1824); *Hypsiboas punctatus* (Schneider, 1799); *Litoria caerulea* (White, 1790); *Osteopilus septentrionalis* (Duméril & Bibron, 1841); *Phyllodytes auratus* (Boulenger, 1917); *Phyllomedusa trinitatis* Mertens, 1926; *Scinax ruber* (Laurenti, 1768); *Smilisca phaeota* (Cope,

1862); *Sphaenorhynchus lacteus* (Daudin, 1801); *Trachycephalus venulosus* (Laurenti, 1768), Craugastoridae: *Pristimantis euphronides* (Schwartz, 1967), Ranidae: *Staurois guttatus* (Günther, 1858), Rhacophoridae: *Rhacophorus pardalis* Gühnter, 1858

**Arachnida: Araneae**, Ctenidae: *Ctenus curvipes* (Keyserling, 1881); *Ctenus sinuatipes* Pickard-Cambridge, 1897; *Ctenus sp. 3* Walckenaer, 1805; *Cupiennius coccineus* Pickard-Cambridge, 1901; *Cupiennius getazi* Simon, 1891; *Cupiennius salei* (Keyserling, 1877); *Phoneutria boliviensis* (Pickard-Cambridge, 1897), Philodromidae: *Philodromus aureolus* (Clerck, 1757); *Philodromus dispar* Walckenaer, 1826, Salticidae: *Evarcha arcuata* (Clerck, 1757); *Marpissa muscosa* (Clerck, 1757); *Salticus scenicus* (Clerck, 1757); *Sitticus pubescens* (Fabricius, 1775); *Pseudeuophrys lanigera* (Simon, 1871), Theraphosidae: *Aphonopelma seemanni* (Pickard-Cambridge, 1897), Thomisidae: *Misumenops spec.*
**Mesostigmata**, Laelapidae: *Androlaelaps schaeferi* (Till, 1969)
**Trombidiformes**, Tetranychidae: *Tetranychus cinnabarinus* Boudreaux, 1956; *Tetranychus urticae* (Koch, 1836)

**Insecta: Blattodea**, Blaberidae: *Gromphadorhina portentosa* (Schaum, 1853); *Nauphoeta cinerea* (Olivier, 1789), Blattellidae: *Blattella germanica* Linnaeus, 1767, Blattidae: *Blatta orientalis* Linnaeus, 1758; *Periplaneta americana* (Linnaeus, 1758); *Periplaneta australasiae* Fabricius, 1775; *Supella supellectilium* (Serville, 1839)
**Coleoptera**, Brentidae: *Cylas puncticollis* (Boheman, 1833), Cantharidae: *Cantharis rustica* Fallén, 1807; *Rhagonycha fulva* Scopoli, 1763, Cerambycidae: *Agrianome Spinicollis* (Macleay, 1827); *Clytus arietis* (Linnaeus, 1758), Chrysomelidae: *Altica lythri* Aubé, 1843; *Cassida canaliculata* Laicharting, 1781; *Chrysolina americana* (Linnaeus, 1758); *Chrysolina fastuosa* Scopoli, 1763; *Chrysolina menthastri* (Suffrian, 1851); *Chrysolina polita* (Linnaeus, 1758); *Clytra quadripunctata* Linnaeus, 1758; *Cryptocephalus spec.* Geoffroy, 1762; *Galerucella nymphaeaei* (Linnaeus, 1758); *Gastrophysa viridula* (De Geer, 1775); *Hemisphaerota cyanea* (Say, 1824); *Leptinotarsa decemlineata* Say, 1824; *Oulema melanopus* (Linnaeus, 1758); *Psylliodes chrysocephalus* (Linnaeus, 1758), Cleridae: *Trichodes alvearius* (Fabricius, 1792), Coccinellidae: *Adalia bipunctata* (Linnaeus, 1758); *Coccinella septempunctata* (Linnaeus, 1758); *Harmonia axyridis* (Pallas, 1773); *Henosepilachna vigintioctopunctata* (Fabricius, 1775); *Psyllobora vigintiduopunctata* (Linnaeus, 1758); *Subcoccinella vigintiquatuorpunctata* (Linnaeus, 1758), Pyrochroidae: *Pyrochroa coccinea* Linnaeus, 1762, Silphidae: *Nicrophorus spec.* Fabricius, 1775
**Dermaptera**, Forficulidae: *Forficula auricularia* Linnaeus, 1758
**Diptera**, Calliphoridae: *Calliphora vicina* Robineau-Desvoidy, 1830; *Calliphora vomitoria* (Linnaeus, 1758); *Lucilia caesar* (Linnaeus, 1758), Syrphidae: *Episyrphus balteatus* (De Geer, 1776); *Eristalis tenax* (Linnaeus, 1758); *Myathropa florea* (Linnaeus, 1758); *Sphaerophoria scripta* (Linnaeus, 1758); *Syrphus ribesii* (Linnaeus, 1758); *Volucella pellucens* (Linnaeus, 1758), Tabanidae: *Tabanus spec* Linnaeus, 1758, Tachinidae: *Tachina fera* (Linnaeus, 1761)
**Hemiptera**, Aphididae: *Aphis fabae* Scopoli, 1763; *Megoura viciae* Buckton, 1876, Cicadellidae: *Aphrodes sp.* Curtis, 1833; *Eupteryx aurata* (Linnaeus, 1758), Coreidae: *Coreus marginatus* (Linnaeus, 1758); *Gonocerus acuteangulatus* (Goeze, 1778); *Leptoglossus occidentalis* Heidemann, 1910, Delphacidae: *Asiraca clavicornis* (Fabricius, 1775); *Javesella pellucida* (Fabricius, 1794); *Ribautodelphax spec* (Ribaut, 1953); *Stenocranus minutus* (Fabricius, 1787), Heterogastridae: *Heterogaster urticae* (Fabricius, 1775), Miridae: *Dicyphus errans* (Wolff, 1804); *Lygocoris pabulinus* (Linnaeus, 1761), Pentatomidae: *Aelia acuminata* (Linnaeus, 1758); *Palomena prasina* (Linnaeus, 1761), Triozidae: *Trioza urticae* (Linnaeus, 1758)

**Hymenoptera**, Formicidae: *Atta cephalotes* (Linnaeus, 1758); *Atta colombica* (Guérin-Méneville, 1844); *Camponotus schmitzi* Stärcke, 1933; *Myrmica scabrinodis* Nylander, 1846; *Oecophylla smaragdina* Fabricius, 1775; *Polyrhachis dives* Smith, 1857, Vespidae: *Vespa crabro* Linnaeus, 1758
**Lepidoptera**, Tortricidae: *Cydia pomonella* (Linnaeus, 1758)
**Mantodea**, Mantidae: *Stagmomantis theophila* Rehn, 1904
**Orthoptera**, Acrididae: *Chorthippus brunneus* (Thunberg, 1815); *Locusta migratoria manilensis* (Linnaeus, 1758), Tettigoniidae: *Conocephalus discolor* (Thunberg, 1815); *Metrioptera roeselii* (Hagenbach, 1822)
**Phasmatodea**, Bacillidae: *Heteropteryx dilatata* (Parkinson, 1798), Diapheromeridae: *Carausius morosus* Sinety, 1901; *Clonaria conformans* (Brunner, 1907), Heteropterygidae: *Trachyaretaon carmelae* Lit & Eusebio, 2005, Phasmatidae: *Eurycantha calcarata* (Lucas, 1869); *Medauroidea extradentata* Brunner, 1907; *Ramulus spec* Saussure, 1862; *Sceptrophasma hispidulum* Wood-Mason, 1873
**Raphidioptera**, Raphidiidae: *Phaeostigma notatum* (Fabricius, 1781)

**Mammalia: Chiroptera**, Myzopodidae: *Myzopoda aurita* Milne-Edwards & A. Grandidier, 1878

**Reptilia: Squamata**, Dactyloidae: *Anolis auratus* Daudin, 1802; *Anolis biporcatus* Wiegmann, 1834; *Anolis capito* (Peters, 1863); *Anolis carolinensis* Voigt, 1832; *Anolis cristatellus* (Duméril & Bibron, 1837); *Anolis cupreus* (Hallowell, 1860); *Anolis distichus* (Cope, 1861); *Anolis equestris* (Merrem, 1820); *Anolis evermanni* (Stejneger, 1904); *Anolis frenatus* (Cope, 1899); *Anolis garmani* (Stejneger, 1899); *Anolis grahami* (Gray, 1845); *Anolis humilis* (Peters, 1863); *Anolis leachi* (Duméril & Bibron, 1837); *Anolis lemurinus* (Cope, 1861); *Anolis limifrons* (Cope, 1871); *Anolis lineatopus* Gray, 1840; *Anolis lionotus* (Cope, 1861); *Anolis pentaprion* (Cope, 1863); *Anolis poecilopus* (Cope, 1862); *Anolis polylepis* (Peters, 1874); *Anolis pulchellus* Duméril & Bibron, 1837; *Anolis sagrei* (Duméril & Bibron, 1837); *Anolis valencienni* (Duméril & Bibron, 1837), Diplodactylidae: *Correlophus ciliatus* Guichenot, 1866, Gekkonidae: *Chondrodactylus bibronii* (Smith, 1846); *Gehyra mutilata* (Wiegmann, 1834); *Gehyra oceanica* (Lesson 1830); *Gehyra vorax* Girard, 1858; *Gekko athymus* Brown & Alcala, 1962; *Gekko gecko* (Linnaeus, 1758); *Gekko gigante* Brown & Alcala, 1978; *Gekko japonicus* (Schlegel, 1836); *Gekko mindorensis* Taylor, 1919; *Gekko monarchus* (Taylor, 1917); *Gekko palawanensis* Taylor, 1925; *Gekko romblon* (Brown & Alcala, 1978); *Gekko Smithii* Gray, 1842; *Gekko subpalmatus* (Günther, 1864); *Gekko swinhonis* Günther 1864; *Gekko vittatus* Houttuyn, 1782; *Hemidactylus frenatus* Schlegel, 1836; *Hemidactylus turcicus* (Linnaeus, 1758); *Lepidodactylus lugubris* (Duméril & Bibron, 1836); *Lepidodactylus pumilus* (Boulenger, 1885); *Phelsuma dubia* (Boettger, 1881); *Phelsuma grandis* Gray, 1870; *Phelsuma laticauda* (Boettger, 1880); *Rhoptropus afer* Peters, 1869; *Rhoptropus barnardi* Hewitt, 1926; *Rhoptropus biporosus* FitzSimons, 1957; *Rhoptropus boultoni* Schmidt, 1933; *Rhoptropus bradfieldi* Hewitt, 1935; *Rhoptropus cf biporosus* (Fitzsimons,1957); *Rhoptropus diporus* Haacke, 1965, Scincidae: *Prasinohaema virens* Peters, 1881; *Prasinohaema prehensicauda* (Loveridge, 1945); *Prasinohaema flavipes* (Parker, 1936); *Lipinia leptosoma* (Brown & Fehlmann, 1958)

# References

[1] Gould SJ (2002) The structure of evolutionary theory. Harvard University Press.

[2] Taylor G, Thomas A (2014) Evolutionary biomechanics: selection, phylogeny, and constraint. Oxford University Press.

[3] McMahon T (1973) Size and shape in biology: Elastic criteria impose limits on biological proportions, and consequently on metabolic rates. Science 179: 1201–1204.

[4] Schmidt-Nielsen K (1975) Scaling in biology: the consequences of size. J Exp Zool 194: 287–307.

[5] McMahon TA, Bonner JT, Freeman W (1983) On size and life. Scientific American Library New York.

[6] Schmidt-Nielsen K (1984) Scaling: why is animal size so important? Cambridge University Press.

[7] LaBarbera M (1990) Principles of design of fluid transport systems in zoology. Science 249: 992–1000.

[8] Weibel ER (1991) Fractal geometry: a design principle for living organisms. Am J Physiol Lung Cell Mol Physiol 261: 361–369.

[9] West GB, Brown JH, Enquist BJ (1999) The fourth dimension of life: fractal geometry and allometric scaling of organisms. Science 284: 1677–1679.

[10] Alexander R, Jayes A, Maloiy G, Wathuta E (1979) Allometry of the limb bones of mammals from shrews (Sorex) to elephant (Loxodonta). J Zool 189: 305–314.

[11] Biewener AA (1989) Scaling body support in mammals: limb posture and muscle mechanics. Science 245: 45–48.

[12] Autumn K, Niewiarowski PH, Puthoff JB (2014) Gecko adhesion as a model system for integrative biology, interdisciplinary science, and bioinspired engineering. Annu Rev Ecol Evol Syst 45: 445-470.

[13] Jagota A, Hui C (2011) Adhesion, friction, and compliance of bio-mimetic and bio-inspired structured interfaces. Mat Sci Eng R 72: 253–292.

[14] Bartlett M, Croll A, King D, Paret B, Irschick D, et al. (2012) Looking beyond fibrillar features to scale gecko-like adhesion. Adv Mater 24: 1078–83.

[15] Hawkes EW, Eason EV, Asbeck AT, Cutkosky MR (2013) The gecko's toe: scaling directional adhesives for climbing applications. IEEE/ASME Trans Mechatronics 18: 518–526.

[16] Labonte D, Federle W (2015) Scaling and biomechanics of surface attachment in climbing animals. Phil Trans R Soc B 370: 20140027.

[17] Pagel M (1999) Inferring the historical patterns of biological evolution. Nature 401: 877–884.

[18] Egset C, Hansen T, Le Rouzic A, Bolstad G, Rosenqvist G, et al. (2012) Artificial selection on allometry: change in elevation but not slope. J Evol Biol 25: 938–948.

[19] Pelabon C, Firmat C, Bolstad GH, Voje KL, Houle D, et al. (2014) Evolution of morphological allometry. Ann NY Acad Sci 1320: 58–75.

[20] Macrini TE, Irschick DJ, Losos JB (2003) Ecomorphological differences in toepad characteristics between mainland and island anoles. J Herpetol 37: 52–58.

[21] Betz O (2003) Structure of the tarsi in some *Stenus* species (Coleoptera, Staphylinidae): External morphology, ultrastructure, and tarsal secretion. J Morphol 255: 24–43.

[22] Wolff JO, Gorb SN (2014) Adhesive foot pads-an adaptation to climbing? An ecological survey in hunting spiders. Zoology 118: 1–7.

[23] Russell AP, Higham TE (2009) A new angle on clinging in geckos: incline, not substrate, triggers the deployment of the adhesive system. ProcR Soc B 276: 3705–3709.

[24] Collins CE, Russell AP, Higham TE (2014) Subdigital adhesive pad morphology varies in relation to structural habitat use in the Namib Day Gecko. Funct Ecol 29: 66–77.

[25] Düllman W, Trüb L (1997) Biology of amphibians. Johns Hopkins University Press, 2nd edition.

[26] Beutel RG, Gorb SN (2001) Ultrastructure of attachment specializations of Hexapods (Arthropoda): Evolutionary patterns inferred from a revised ordinal phylogeny. J Zool Syst Evol Res 39: 177–207.

[27] Gamble T, Greenbaum E, Jackman TR, Russell AP, Bauer AM (2012) Repeated origin and loss of adhesive toepads in geckos. PLoS One 7: e39429.

[28] Wolff JO, Nentwig W, Gorb SN (2013) The great silk alternative: Multiple co-evolution of web loss and sticky hairs in spiders. PLoS One 8: e62682.

[29] Johnson MK, Russell AP (2009) Configuration of the setal fields of *Rhoptropus* (gekkota: Gekkonidae): functional, evolutionary, ecological and phylogenetic implications of observed pattern. J Anat 214: 937–955.

[30] Higham TE, Birn-Jeffery AV, Collins CE, Hulsey CD, Russell AP (2014) Adaptive simplification and the evolution of gecko locomotion: Morphological and biomechanical consequences of losing adhesion. PNAS 112: 809–814.

[31] Schmidt-Nielsen K (1970) Energy metabolism, body size, and problems of scaling. Fed Proc 29: 1524–1532.

[32] Powell GL, Russell AP (1992) Locomotor correlates of ecomorph designation in *Anolis*: an examination of three sympatric species from Jamaica. Can J Zool 70: 725–739.

[33] Du Bois D, Du Bois EF (1916) Clinical calorimetry: tenth paper a formula to estimate the approximate surface area if height and weight be known. Arch Intern Med 17: 863–871.

[34] Smith JM, Barnes WJP, Downie J, Ruxton G (2006) Adhesion and allometry from metamorphosis to maturation in hylid tree frogs: a sticky problem. J Zool 270: 372–383.

[35] Hanna G, Barnes WJP (1991) Adhesion and detachment of the toe pads of tree frogs. J Exp Biol 155: 103–125.

[36] Barnes WJP, Oines C, Smith J (2006) Whole animal measurements of shear and adhesive forces in adult tree frogs: insights into underlying mechanisms of adhesion obtained from studying the effects of size and scale. J Comp Physiol A 192: 1179–1191.

[37] Smith JM, Barnes WJP, Downie JR, Ruxton GD (2006) Structural correlates of increased adhesive efficiency with adult size in the toe pads of hylid tree frogs. J Comp Physiol A 192: 1193–1204.

[38] Crawford N, Endlein T, Barnes WJP (2012) Self-cleaning in tree frog toe pads; a mechanism for recovering from contamination without the need for grooming. J Exp Biol 215: 3965–3972.

[39] Arzt E, Gorb S, Spolenak R (2003) From micro to nano contacts in biological attachment devices. PNAS 100: 10603–10606.

[40] Peattie AM, Full RJ (2007) Phylogenetic analysis of the scaling of wet and dry biological fibrillar adhesives. PNAS 104: 18595–18600.

[41] Gorb S, Gorb E, Kastner V (2001) Scale effects on the attachment pads and friction forces in syrphid flies. J Exp Biol 204: 1421–1431.

[42] Federle W (2006) Why are so many adhesive pads hairy? J Exp Biol 209: 2611–2621.

[43] Arnold SJ (1983) Morphology, performance and fitness. Am Zool 23: 347–361.

[44] Roth L, Willis E (1952) Tarsal structure and climbing ability of cockroaches. J Exp Zool 119: 483–517.

[45] Emerson S, Diehl D (1980) Toe pad morphology and mechanisms of sticking in frogs. Biol J Linn Soc 13: 199–216.

[46] Stork N (1980) Experimental analysis of adhesion of *Chrysolina polita* (Chrysomelidae: Coleoptera) on a variety of surfaces. J Exp Biol 88: 91–107.

[47] Green D, Alberch P (1981) Interdigital webbing and skin morphology in the neotropical salamander genus Bolitoglossa (Amphibia; Plethodontidae). J Morphol 170: 273–282.

[48] Walker G, Yulf AB, Ratcliffe J (1985) The adhesive organ of the blowfly, *Calliphora vomitoria*: a functional approach (Diptera: Calliphoridae). J Zool 205: 297–307.

[49] Bauer AM, Good D (1986) Scaling of scansorial surface area in the genus Gekko. In: Roček Z, editor, Studies in herpetology, Prague: Charles University. pp. 363–366.

[50] Ishii S (1987) Adhesion of a leaf-feeding ladybird *Epilachna vigintioctomaculata* (Coleoptera, Coccinellidae) on a vertically smooth surface. Appl Entomol Zool 22: 222–228.

[51] Lees AD, Hardie J (1988) The organs of adhesion in the aphid *Megoura viciae*. J Exp Biol 136: 209–228.

[52] Dixon AFG, Croghan P, Gowing R (1990) The mechanism by which aphids adhere to smooth surfaces. J Exp Biol 152: 243–253.

[53] Walker G (1993) Adhesion to smooth surfaces by insects–a review. Int J Adhes Adhes 13: 3–7.

[54] Irschick DJ, Austin CC, Petren K, Fisher RN, Losos JB, et al. (1996) A comparative analysis of clinging ability among pad-bearing lizards. Biol J Linn Soc 59: 21–35.

[55] Eisner T, Aneshansley D (2000) Defense by foot adhesion in a beetle (*Hemisphaerota cyanea*). PNAS 97: 6568–6573.

[56] Federle W, Rohrseitz K, Hölldobler B (2000) Attachment forces of ants measured with a centrifuge: better 'wax-runners' have a poorer attachment to a smooth surface. J Exp Biol 203: 505–512.

[57] Gorb SN, Beutel RG, Gorb EV, Jiao Y, Kastner V, et al. (2002) Structural design and biomechanics of friction-based releasable attachment devices in insects. Integr Comp Biol 42: 1127–1139.

[58] Kesel A, Martin A, Seidl T (2004) Getting a grip on spider attachment: an afm approach to microstructure adhesion in arthropods. Smart Mater Struct 13: 512.

[59] Elstrott J, Irschick DJ (2004) Evolutionary correlations among morphology, habitat use and clinging performance in caribbean *Anolis* lizards. Biol J Linn Soc 83: 389–398.

[60] Federle W, Baumgartner W, Hölldobler B (2004) Biomechanics of ant adhesive pads: frictional forces are rate- and temperature dependent. J Exp Biol 206: 67–74.

[61] Frantsevich L, Gorb S (2004) Structure and mechanics of the tarsal chain in the hornet, *Vespa crabro* (Hymenoptera: Vespidae): implications on the attachment mechanism. Arthropod Struct Dev 33: 77 – 89.

[62] Zahn M (2006) Allometrie der Hafthaarmorphologie bei Arthropoden. Master's thesis, Universität Würzburg.

[63] Bohn HF (2007) Biomechanik von Insekten-Pflanzen-Interaktionen bei Nepenthes-Kannenpflanzen. Ph.D. thesis, Julius-Maximilians-Universität Würzburg.

[64] Voigt D, Gorb E, Gorb S (2007) Plant surface-bug interactions: *Dicyphus errans* stalking along trichomes. Arthropod Plant Interact 1: 221–243.

[65] Clemente CJ, Federle W (2008) Pushing versus pulling: division of labour between tarsal attachement pads in cockroaches. Proc R Soc B 275: 1329–1336.

[66] Drechsler P (2008) Mechanics of adhesion and friction in stick insects and tree frogs. Ph.D. thesis, Julius-Maximilians-Universität Würzburg.

[67] Niewiarowski PH, Lopez S, Ge L, Hagan E, Dhinojwala A (2008) Sticky gecko feet: the role of temperature and humidity. PLoS One 3: e2192.

[68] Frantsevich L, Ji A, Dai Z, Wang J, Frantsevich L, et al. (2008) Adhesive properties of the arolium of a lantern-fly, *Lycorma delicatula* (Auchenorrhyncha, Fulgoridae). J Insect Physiol 54: 818–827.

[69] Al Bitar L, Voigt D, Zebitz C, Gorb S (2009) Tarsal morphology and attachment ability of the codling moth *Cydia pomonella* L.(Lepidoptera, Tortricidae) to smooth surfaces. J Insect Physiol 55: 1029–1038.

[70] Bullock JMR, Federle W (2009) Division of labour and sex differences between fibrillar, tarsal adhesive pads in beetles: effective elastic modulus and attachment performance. J Exp Biol 212: 1876–1888.

[71] Geiselhardt SF, Federle W, Prüm B, Geiselhardt S, Lamm S, et al. (2009) Impact of chemical manipulation of tarsal liquids on attachment in the Colorado potato beetle, *Leptinotarsa decemlineata*. J Insect Physiol 56: 398–404.

[72] Lüken D, Voigt D, Gorb S, Zebitz C (2009) Die Tarsenmorphologie und die Haftfähigkeit des Schwarzen Batatenkäfers *Cylas puncticollis* (Boheman) auf glatten oberflächen mit unterschiedlichen physiko-chemischen eigenschaften. Mitt Dtsch Ges allg angew Entomol 17: 109–113.

[73] Webster NB, Johnson MK, Russell AP (2009) Ontogenetic scaling of scansorial surface area and setal dimensions of *Chondrodactylus bibronii* (Gekkota: Gekkonidae): testing predictions derived from cross-species comparisons of gekkotans. Acta Zool 90: 18–29.

[74] Gorb EV, Hosoda N, Miksch C, Gorb SN (2010) Slippery pores: anti-adhesive effect of nanoporous substrates on the beetle attachment system. J R Soc Interface 7: 1571–1579.

[75] Riskin D, Racey P (2010) How do sucker footed bats hold on, and why do they roost head up? Biol J Linn Soc 99: 233–240.

[76] Varenberg M, Pugno N, Gorb S (2010) Spatulate structures in biological fibrillar adhesion. Soft Matter 6: 3269–3272.

[77] Orchard MJ, Kohonen M, Humphries S (2012) The influence of surface energy on the self-cleaning of insect adhesive devices. J Exp Biol 215: 279–286.

[78] Orchard MJ (2012) The functional morphology of insect adhesive devices and its implications for ecology. Ph.D. thesis, University of Hull.

[79] Voigt D, Schweikart A, Fery A, Gorb S (2012) Leaf beetle attachment on wrinkles: isotropic friction on anisotropic surfaces. J Exp Biol 215: 1975–1982.

[80] Wolff JO, Gorb SN (2012) Surface roughness effects on attachment ability of the spider *Philodromus dispar* (Araneae, Philodromidae). J Exp Biol 215: 179–184.

[81] Anyon MJ (2013) A Multi-Disciplinary Study of Insect Adhesion: Functional Biomechanics and Applications. Ph.D. thesis, University of Hull.

[82] Endlein T, Barnes WJP, Samuel DS, Crawford NA, Biaw AB, et al. (2013) Sticking under wet conditions: The remarkable attachment abilities of the torrent frog, *Staurois guttatus*. PloS One 8: e73810.

[83] Labonte D, Federle W (2013) Functionally different pads on the same foot allow control of attachment: stick insects have load-sensitive "heel" pads for friction and shear-sensitive "toe" pads for adhesion. PLoS One 8: e81943.

[84] Crandell KE, Herrel A, Sasa M, Losos JB, Autumn K (2014) Stick or grip? Co-evolution of adhesive toepads and claws in *Anolis* lizards. Zoology 117: 363–369.

[85] Grohmann C, Blankenstein A, Koops S, Gorb SN (2014) Attachment of *Galerucella nymphaeae* (Coleoptera, Chrysomelidae) to surfaces with different surface energy. J Exp Biol 217: 4213–4220.

[86] Lapinski W, Walther P, Tschapka M (2015) Morphology reflects microhabitat preferences in an assemblage of neotropical wandering spiders. Zoomorphology 134: 219–236.

[87] Luff M (2007) The Carabidae (ground beetles) of Britain and Ireland. RES handbooks for the identification of British Insects, volume 4. Field Studies Council, Shrewsbury.

[88] Biedermann R, Niedringhaus R (2009) The plant- and leafhoppers of Germany: identification key to all species. Scheeßel: Wissenschaftlich Akademischer Buchvertrieb–Fründ.

[89] Kunz G, Nickel H, Niedringhaus R (2011) Fotoatlas der Zikaden Deutschlands. Scheeßel: Wissenschaftlich Akademischer Buchvertrieb–Fründ.

[90] Schneider C, Rasband W, Eliceiri K (2012) NIH Image to ImageJ: 25 years of image analysis. Nat Methods 9: 671–675.

[91] Bullock JMR, Drechsler P, Federle W (2008) Comparison of smooth and hairy attachment pads in insects: friction, adhesion and mechanisms for direction-dependence. J Exp Biol 211: 3333–3343.

[92] Autumn K, Gravish N (2008) Gecko adhesion: evolutionary nanotechnology. Phil Trans R Soc A 366: 1575–1590.

[93] Bullock JMR, Federle W (2011) Beetle adhesive hairs differ in stiffness and stickiness: *in vivo* adhesion measurements on individual setae. Naturwissenschaften 98: 381–387.

[94] Peattie AM, Dirks JH, Henriques S, Federle W (2011) Arachnids secrete a fluid over their adhesive pads. PLoS One 6: e20485.

[95] Arnold J (1974) Adaptive features on the tarsi of cockroaches (Insecta: Dictyoptera). Insect Morphol Embryol 3: 317–334.

[96] Frazier SF, Larsen GS, Neff D, Quimby L, Carney M, et al. (1999) Elasticity and movements of the cockroach tarsus in walking. J Comp Physiol 185: 157–172.

[97] Beutel R, Gorb S (2006) A revised interpretation of attachment structures in Hexapoda with special emphasis on Mantophasmatodea. Arthropod Syst Phylogeny 64: 3–25.

[98] Eberhard MJ, Pass G, Picker MD, Beutel R, Predel R, et al. (2009) Structure and function of the arolium of Mantophasmatodea (Insecta). J Morphol 270: 1247–1261.

[99] Clemente C, Dirks J, Barbero D, Steiner U, Federle W (2009) Friction ridges in cockroach climbing pads: anisotropy of shear stress measured on transparent, microstructured substrates. J Comp Physiol A 195: 805–814.

[100] Labonte D, Williams J, Federle W (2014) Surface contact and design of fibrillar 'friction pads' in stick insects (*carausius morosus*): mechanisms for large friction coefficients and negligible adhesion. J R Soc Interface 11: 20140034.

[101] Gorb S, Scherge M (2000) Biological microtribology: anisotropy in frictional forces of orthopteran attachment pads reflects the ultrastructure of a highly deformable material. Proc R Soc B 267: 1239–1244.

[102] Grohmann C, Henze MJ, Nørgaard T, Gorb SN (2015) Two functional types of attachment pads on a single foot in the Namibia bush cricket *Acanthoproctus diadematus* (Orthoptera: Tettigoniidae). Proc R Soc B 282.

[103] Drotlef DM, Appel E, Peisker H, Dening K, del Campo A, et al. (2014) Morphological studies of the toe pads of the rock frog, *Staurois parvus* (family: Ranidae) and their relevance to the development of new biomimetically inspired reversible adhesives. Interface Focus 5: 20140036.

[104] Emerson SB S (1991) The ecomorphology of bornean tree frogs (family Rhacophoridae). Zool J Linn Soc 101: 337–357.

[105] Voigt D, Schuppert J, Dattinger S, Gorb S (2008) Sexual dimorphism in the attachment ability of the colorado potato beetle *Leptinotarsa decemlineata* (Coleoptera: Chrysomelidae) to rough substrates. J Insect Physiol 54: 765–776.

[106] Al Bitar L, Voigt D, Zebitz CP, Gorb SN (2010) Attachment ability of the codling moth *Cydia pomonella* L. to rough substrates. J Insect Physiol 56: 1966–1972.

[107] Labonte D, Federle W (2015) Rate-dependence of 'wet' biological adhesives and the function of the pad secretion in insects. Soft Matter 11: 8661–8673.

[108] Schluter D (1996) Adaptive radiation along genetic lines of least resistance. Evolution 50: 1766–1774.

[109] Pyron RA, Wiens JJ (2011) A large-scale phylogeny of Amphibia including over 2800 species, and a revised classification of extant frogs, salamanders, and caecilians. Mol Phylogenet Evol 61: 543–583.

[110] Pyron RA, Burbrink FT, Wiens JJ (2013) A phylogeny and revised classification of Squamata, including 4161 species of lizards and snakes. BMC Evol Biol 13: 93.

[111] Misof B, Liu S, Meusemann K, Peters RS, Donath A, et al. (2014) Phylogenomics resolves the timing and pattern of insect evolution. Science 346: 763–767.

[112] Grandcolas P (1996) The phylogeny of cockroach families: a cladistic appraisal of morpho-anatomical data. Can J Zool 74: 508–527.

[113] Bocak L, Barton C, Crampton-Platt A, Chesters D, Ahrens D, et al. (2014) Building the Coleoptera tree-of-life for > 8000 species: composition of public DNA data and fit with linnean classification. Syst Entomol 39: 97–110.

[114] Wiegmann BM, Trautwein MD, Winkler IS, Barr NB, Kim JW, et al. (2011) Episodic radiations in the fly tree of life. PNAS 108: 5690–5695.

[115] Hua J, Li M, Dong P, Cui Y, Xie Q, et al. (2008) Comparative and phylogenomic studies on the mitochondrial genomes of Pentatomomorpha (Insecta: Hemiptera: Heteroptera). BMC genomics 9.

[116] Cryan JR, Urban JM (2012) Higher-level phylogeny of the insect order Hemiptera: is Auchenorrhyncha really paraphyletic? Syst Entomol 37: 7–21.

[117] Astruc C, Julien J, Errard C, Lenoir A (2004) Phylogeny of ants (Formicidae) based on morphology and DNA sequence data. Mol Phylogenet Evol 31: 880–893.

[118] tolweborg (accessed March 2015). Tree of Life Project.

[119] Hansen TF, Pienaar J, Orzack SH (2008) A comparative method for studying adaptation to a randomly evolving environment. Evolution 62: 1965–1977.

[120] Voje KL, Hansen TF (2013) Evolution of static allometries: adaptive change in allometric slopes of eye span in stalk-eyed flies. Evolution 67: 453–467.

[121] Paradis E (2013) Molecular dating of phylogenies by likelihood methods: a comparison of models and a new information criterion. Mol Phylogenet Evol 67: 436–444.

[122] Revell LJ (2010) Phylogenetic signal and linear regression on species data. Methods Ecol Evol 1: 319–329.

[123] Paradis E, Claude J, Strimmer K (2004) APE: Analyses of phylogenetics and evolution in r language. Bioinformatics 20: 289–290.

[124] Revell LJ (2012) phytools: an R package for phylogenetic comparative biology (and other things). Methods Ecol Evol 3: 217–223.

[125] Harvey PH, Pagel MD (1991) The comparative method in evolutionary biology, volume 239. Oxford: Oxford University Press.

[126] Warton DI, Wright IJ, Falster DS, Westoby M (2006) Bivariate line-fitting methods for allometry. Biol Rev 81: 259–291.

[127] Hansen TF, Bartoszek K (2012) Interpreting the evolutionary regression: the interplay between observational and biological errors in phylogenetic comparative studies. Syst Biol 61: 413–425.

[128] Revell LJ (2013) Two new graphical methods for mapping trait evolution on phylogenies. Methods Ecol Evol 4: 754–759.